



Article

Phylogenetic and Expression Analysis of Fos Transcription Factors in Zebrafish

Khadizatul Kubra ¹, Gurveer K. Gaddu ¹, Clifford Liongue ^{1,2} , Somayyeh Heidary ¹, Alister C. Ward ^{1,2}, Amardeep S. Dhillon ^{1,2,3,4,*} and Faiza Basheer ^{1,2,*}

¹ School of Medicine, Deakin University, Geelong, VIC 3216, Australia

² Institute of Mental and Physical Health and Clinical Translation, Deakin University, Geelong, VIC 3216, Australia

³ Olivia Newton-John Cancer Research Institute, Melbourne, VIC 3084, Australia

⁴ School of Cancer Medicine, LaTrobe University, Melbourne, VIC 3086, Australia

* Correspondence: amardeep.dhillon@deakin.edu.au (A.S.D.); faiza.basheer@deakin.edu.au (F.B.)

Abstract: Members of the FOS protein family regulate gene expression responses to a multitude of extracellular signals and are dysregulated in several pathological states. Whilst mouse genetic models have provided key insights into the tissue-specific functions of these proteins in vivo, little is known about their roles during early vertebrate embryonic development. This study examined the potential of using zebrafish as a model for such studies and, more broadly, for investigating the mechanisms regulating the functions of Fos proteins in vivo. Through phylogenetic and sequence analysis, we identified six zebrafish FOS orthologues, *fosaa*, *fosab*, *fosb*, *fosl1a*, *fosl1b*, and *fosl2*, which show high conservation in key regulatory domains and post-translational modification sites compared to their equivalent human proteins. During embryogenesis, zebrafish *fos* genes exhibit both overlapping and distinct spatiotemporal patterns of expression in specific cell types and tissues. Most *fos* genes are also expressed in a variety of adult zebrafish tissues. As in humans, we also found that expression of zebrafish FOS orthologs is induced by oncogenic BRAF-ERK signalling in zebrafish melanomas. These findings suggest that zebrafish represent an alternate model to mice for investigating the regulation and functions of Fos proteins in vertebrate embryonic and adult tissues, and cancer.

Keywords: Fos; activator protein-1; transcription factor; embryogenesis; zebrafish; development; ortholog



Citation: Kubra, K.; Gaddu, G.K.; Liongue, C.; Heidary, S.; Ward, A.C.; Dhillon, A.S.; Basheer, F. Phylogenetic and Expression Analysis of Fos Transcription Factors in Zebrafish. *Int. J. Mol. Sci.* **2022**, *23*, 10098. <https://doi.org/10.3390/ijms231710098>

Academic Editors: Cheol-Hee Kim and Seong-kyu Choe

Received: 21 August 2022

Accepted: 30 August 2022

Published: 3 September 2022

Publisher's Note: MDPI stays neutral with regard to jurisdictional claims in published maps and institutional affiliations.



Copyright: © 2022 by the authors. Licensee MDPI, Basel, Switzerland. This article is an open access article distributed under the terms and conditions of the Creative Commons Attribution (CC BY) license (<https://creativecommons.org/licenses/by/4.0/>).

1. Introduction

The mammalian FOS proteins, c-FOS, FOSB, FOSL1, and FOSL2, belong to the activator protein-1 (AP-1) family of transcription factors that contain evolutionarily conserved basic leucine zipper (bZIP) domains [1]. FOS proteins regulate transcription by forming heterodimers with other AP-1 proteins, particularly members of the JUN, ATF, and MAF families [2–5]. AP-1 complexes regulate the expression of genes important for cell proliferation, differentiation, and apoptosis in response to a plethora of extracellular signals, including growth factors, cytokines, and hormones [3,5–11]. In addition to possessing a conserved basic leucine zipper (bZIP) domain mediating DNA binding and dimerisation, FOS isoforms have different N-terminal and C-terminal regions, providing a basis for their differential regulation and functional activities [1]. c-FOS and FOSB have N- and C-terminal transactivation motifs termed the N-TA, C-TM, and TBD that are absent in FOSL1 and FOSL2. Additional C-terminal motifs HOB1 and HOB2, which stabilise and facilitate assembly of the pre-initiation complex, are present solely in c-FOS [1,12,13]. In contrast, FOSB has a unique proline-rich functional module, PRM also within the C-terminal region [14]. Another critical regulatory region present in all FOS proteins is the C-terminal destabilising element (C-DEST). Phosphorylation of this domain is induced by ERK MAPK signalling and leads to protein stabilisation [15–17].

FOS family members are implicated with the pathogenesis of various diseases [18]. Aberrant expression and activation of FOS proteins is driven by dysregulation of key cancer-associated signalling pathways, most notably the ERK MAPK pathway [1]. The pro-tumorigenic actions of FOS family members have been examined in a variety of in vitro and in vivo models, which have identified roles for FOS proteins in oncogenic transformation [19] and cancer progression [20–23]. Early studies showed that rodent fibroblasts undergo transformation upon expression of c-FOS but not FOSL1 and FOSL2, which is attributed to differences in the N- and C-terminal regions of these proteins. Notably, c-FOS and FOSB harbour transactivation domains that are absent in FOSL1 and FOSL2 [1,12]. Consequently, AP-1 dimers containing c-FOS and FOSB show stronger transcription activation potential than those containing FOSL1 and FOSL2 [24,25].

Genetic knockout and transgenic mouse models have shown that individual Fos proteins have specific in vivo functions [26,27]. *c-Fos* deficiency perturbs normal development of bone, cartilage, and the haematopoietic system [28], whereas its transgenic expression in the bone induces the formation of osteosarcoma [29]. *Fosb* deficiency impairs brain development, leading to nurturing defects in the adult female mouse, while transgenic overexpression of *Fosb2* in the thymus disrupts T-cell differentiation [30]. Deficiency of either *Fosl1* and *Fosl2* in mice caused embryonic lethality, while their overexpression resulted in abnormalities in bone and ocular development [3,27]. *Fosl1* deletion also led to placental defects associated with the aberrant differentiation of trophoblasts [31,32].

Despite providing important insights into the in vivo functions of specific FOS proteins in normal and disease states, the use of mouse models to investigate the mechanisms regulating the activities of individual FOS isoforms in vivo is challenging. In addition, mouse models have provided limited insight into the functions of FOS isoforms during early vertebrate development. The zebrafish has emerged as a robust in vivo model for early developmental studies, as its embryos are transparent and develop externally, facilitating easy observation of key processes [33]. The zebrafish genome has been sequenced and about 70% of human genes have at least one ortholog in zebrafish. In addition, their rapid development, high fecundity, low maintenance costs, and amenability to genetic manipulation, including tissue-specific targeted genome editing and transgenesis, makes them well suited for investigating molecular mechanisms in vivo. Through phylogenetic and sequence analysis, we identified six zebrafish FOS homologues, *fosaa*, *fosab*, *fosb*, *fosl1a*, *fosl1b*, and *fosl2*, which encoded proteins showing high sequence conservation in key regulatory domains and post-translational modification sites compared to the equivalent human proteins. Spatiotemporal expression analysis revealed both overlapping and distinct patterns of *fos* gene in specific cell types and tissues during early embryonic development. Our data thus suggest that the zebrafish represents a valuable vertebrate model for investigating Fos protein regulation in vivo and defining their functions during embryogenesis.

2. Results

2.1. Identification of Zebrafish Fos Proteins

The human FOS gene family consists of FOS, FOSB, FOSL1, and FOSL2 [1]. Analysis of genomic databases identified six zebrafish FOS genes, which synteny analysis indicated were single *fosb* and *fosl2* orthologues, but duplicated *fosaa/fosab* and *fosl1a/fosl1b* paralogues (Figure 1). Phylogenetic analysis of the encoded proteins showed they formed a distinct clade from another bZIP transcription factor (JDP2) outgroup (Figure 2) [34,35]. Within the FOS clades, there was a clear sub-clade for c-FOS, FOSB, and FOSL2 proteins, with the c-FOS paralogue *Fosaa* being more divergent than *Fosab*. In contrast, while *Fosl1a* grouped with its mammalian counterparts, *Fosl1b* sat as an outlier to all subclades. In addition, clades of c-FOS and FOSB as well as FOSL1 and FOSL2 proteins were grouped under two separate clades, indicating that these pairs of proteins share a common ancestral origin.

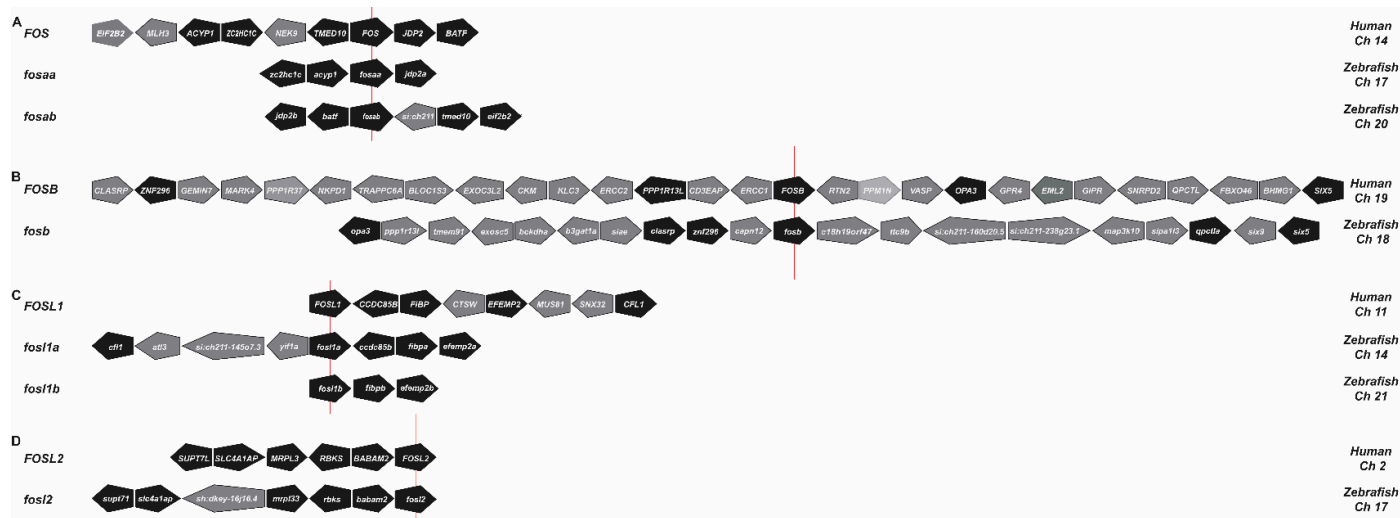


Figure 1. Synteny analysis of *FOS* genes. Human and zebrafish *FOS* (A), *FOSB* (B), *FOSL1* (C), and *FOSL2* (D) gene loci, indicating adjacent genes in their respective orientations. Zebrafish genes that share conserved synteny between human neighbouring genes are shown in black and non-syntenic genes in grey. The red line indicates the reference gene. Ch, chromosome.

2.2. Major Functional Domains and Post-Translationally Modified Residues in Human *FOS* Proteins Are Conserved in Their Zebrafish Counterparts

Sequence alignment of full-length human, mouse, and zebrafish *FOS* proteins revealed that, in addition to the bZIP domain, other major N- and C-terminal functional domains of human *FOS* proteins [1] were present in their corresponding zebrafish proteins (Figures 3 and S1). Protein BLAST analysis showed that human c-*FOS* was 48% identical to *Fosaa* and 55% to *Fosab*. For c-*FOS*, regions of significant homology were present throughout the protein, particularly in the bZIP motif, and to a lesser extent in the C- and N-terminal transactivation domains, N-TA, HOB1, HOB2, C-TM, and TBD (Figures 3A and S1A). Notably, previously characterised regulatory phosphorylation sites in mammalian *FOS* proteins are highly conserved in zebrafish *Fosab* but not in *Fosaa*, where only the C-terminal phosphorylation sites were conserved. The region of highest conservation in the c-*FOS* paralogs was the bZIP domain, while the C-DEST region of *Fosab* was more conserved to c-*FOS* than that of *Fosaa* (Figure S1A).

The overall sequence identity of zebrafish *FosB* and human *FOSB* was 65%, with the bZIP domain being 93% identical. Amongst *FOS* proteins, *FosB* showed the highest overall sequence and bZIP domain conservation. Zebrafish *FosB* showed high conservation of the bZIP motif with mammalian *FOSB* and moderate conservation of the C- and N-terminal transactivation domains (N-TA, PRM, C-TM, and TBM) (Figures 3B and S1B). Key regulatory phosphorylation sites in human *FOSB* were also conserved in its zebrafish ortholog. However, the C-DEST region in zebrafish *FosB* is least conserved amongst *FOS* proteins.

In contrast to c-*FOS* and *FOSB*, human *FOSL1* and *FOSL2* lack potent transactivation domains [1,12]. The overall sequence identities of *Fosl1a* and *Fosl1b* compared to human *FOSL1* are 49% and 40%, respectively, with their bZIP domain identities being 78% and 59%, respectively (Figure 3C). Finally, zebrafish *Fosl2* showed 65% overall identity and 85% bZIP domain identity compared to human *FOSL2* (Figure 3D). Of the two zebrafish *FOSL1* paralogs, *Fosl1b* showed weaker sequence conservation compared to *Fosl1a*, with *Fosl1b* lacking the C-DEST domain and C-terminal phosphorylation sites (Figures 3C and S1C). Amongst *FOS* proteins, the C-DEST domain of zebrafish *Fosl2* showed highest identity to the human protein (Figure S1D). Collectively, these findings suggest that zebrafish and human *FOS* proteins share key functional and regulatory features.

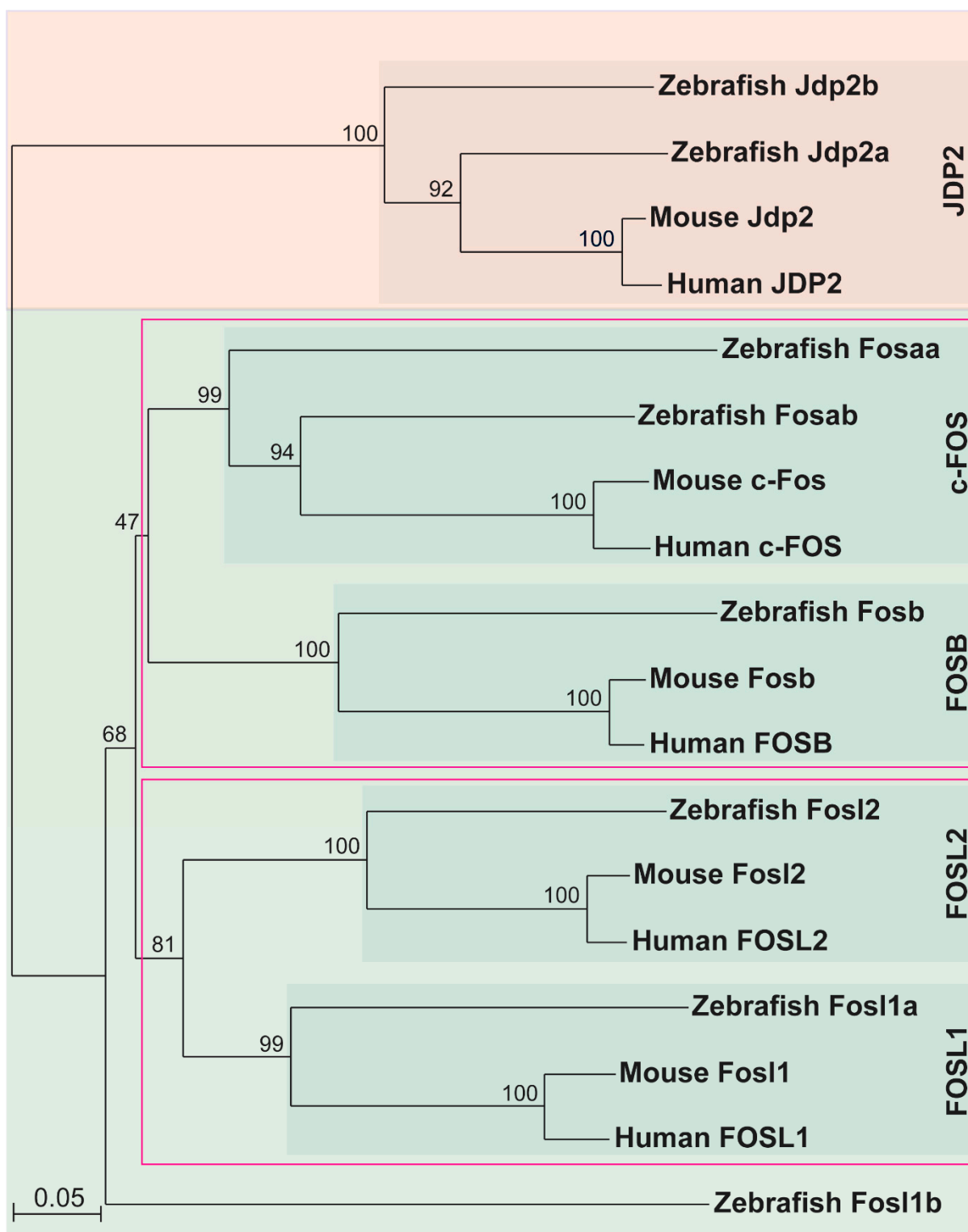


Figure 2. Phylogeny of mammalian and zebrafish FOS proteins. Phylogenetic analysis of human, mouse, and zebrafish FOS proteins were performed using the neighbour-joining algorithm and visualised with TreeView, with bootstrap values represented as a percentage of 1000 replicates and the relative evolutionary distance represented at the bottom left corner. JDP2 proteins were used as a closely related outgroup. Clades of related proteins are indicated within pink coloured boxes.

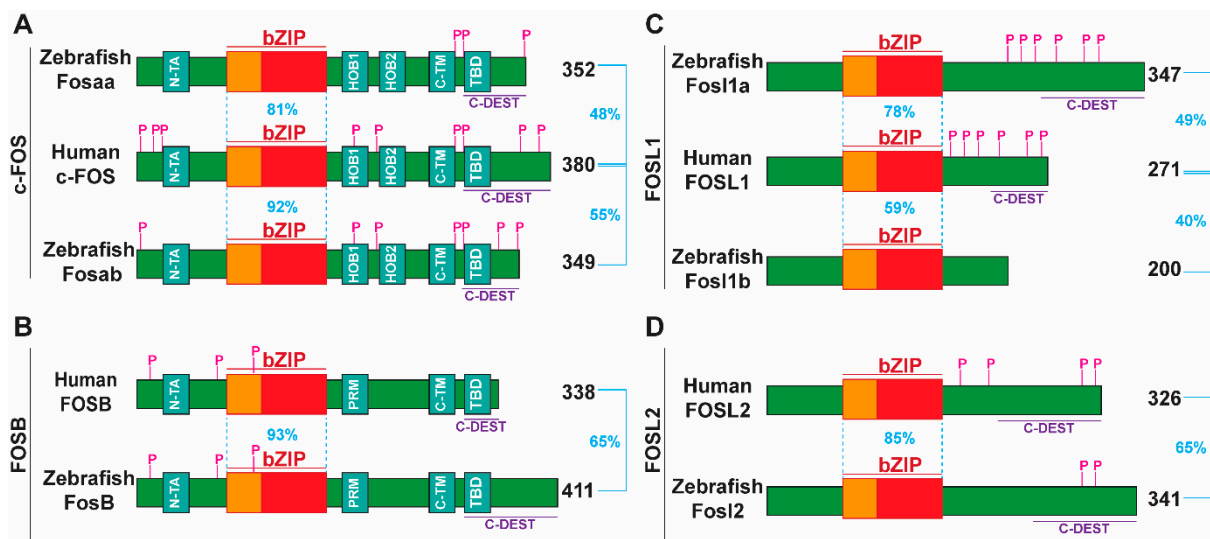


Figure 3. Schematic representation of human and zebrafish FOS proteins. Depicted are human and zebrafish sequences related to c-FOS (A), FOSB (B), FOSL1 (C), and FOSL2 (D). Functional regions indicated are the basic leucine zipper (bZIP) including the basic region for DNA interaction (orange box) and leucine zipper for dimerization (red box), N-terminal transactivation domain (N-TA), homology box one and two (HOB1, HOB2), proline-rich motif (PRM), C-terminal transactivation motif (C-TM), transactivation domain (TBD), and destabiliser region (C-DEST). Previously characterised phosphorylation (P) sites curated in the Phosphosite database ([phosphosite.org](https://www.phosphosite.org) (accessed on 24 July 2022)) are indicated. The percentage identity within the bZIP domain and overall protein are indicated by blue dotted or solid lines and text, with the protein length indicated on the left in black text.

2.3. Zebrafish Fos Genes Show Distinct Expression Patterns during Embryonic Development

Wholemount in situ hybridisation (WISH) analysis was used to establish the pattern of expression of each zebrafish Fos isoform during early embryonic development. Maternal *fosaa* transcripts were detected in 1-cell embryos (0 hpf), and by 12 hpf (6-somite stage), zygotic expression was observed in the brain (forebrain, midbrain, and hindbrain), pre-somitic mesoderm, somites, and tailbud (Figure 4A), and at 24 hpf, in the brain (forebrain, midbrain, and hindbrain), eye, migratory neural crest cells, melanoblasts, and notochord (Figure 5A,A'). From 48 hpf to 4 dpf, no specific *fosaa* expression was observed compared to the sense controls (Figures 5B–C' and S2). These results suggest a role for *fosaa* during early organ development (brain, eye) and formation of diverse cell lineages including melanocytes, smooth muscle, craniofacial bone and cartilage, cranial neurons, and glia. The pattern of *fosab* expression was similar to *fosaa* in early embryos (Figure 4B) but persisted until 4 dpf in multiple regions of the embryo (Figure 5D–F'). These included the brain, eyes, migrating neural crest cells, melanoblasts, epidermis, liver, and pancreas at 24 hpf (Figures 5D,D' and S4A–C), and the brain, heart, gut, migratory neural crest cells, lateral line neuromasts, nephron (proximal straight tubule of nephron and distal early of nephron), cloaca, somites, and tailbud at 48 hpf (Figures 5E,E' and S4D–F), while at 4 dpf, it was expressed in the mouth, otic vesicle, peridermis, epidermis, jaws, pharyngeal arch, and caudal fin (Figures 5F,F' and S4G–K). These observations suggest a role for *fosab* during the development of multiple organs (eye, brain, heart, liver, and pancreas) and cell lineages (e.g., melanocytes and epidermal cells).

Zebrafish *fosb* was expressed from 8 hpf (75% epiboly stage) (Figure 4C), with specific expression observed in the hatching gland and eye at 24 hpf (Figure 5G,G'). At 48 hpf, *fosb* expression was present in the brain (midbrain, pallium), heart, hatching gland, and tailbud (Figures 5H,H' and S4L–N), while at 4 dpf, expression was also observed in the otic vesicle, pharyngeal arches, epidermis, and caudal fin, including the fin rays (Figures 5I,I' and S4O,P).

Zebrafish *fos11a* transcripts were not detected at early time points, but were observed in the forebrain, pancreas, and tailbud at 24 hpf (Figure 5J,J') and in the eye, brain, peridermis, and pectoral fin bud at 48 hpf (Figures 5K,K' and S4Q–T), whereas no specific *fos11a* expression was detected at 4 dpf (Figure 5L,L'). Compared to *fos11a*, *fos11b* exhibits very limited expression, which was maternally deposited at the one cell stage (0 hpf) (Figure 4E). At 24 hpf, *fos11b* expression was localised to the hatching gland (Figure 5M,M'), while at 48 hpf, it was expressed in the hindbrain and peridermis (Figure 5N,N'). Thus, *fos11b* may play specific roles in the development of the brain, epidermis, and hatching gland.

Zebrafish *fosl2* showed the highest early embryonic expression being detected at 12 hpf in the eyes, somites, presomitic mesoderm, mid and hindbrain, and tailbud (Figure 4F). At 24 hpf, *fosl2* was expressed in the brain (forebrain, midbrain, hindbrain, and midbrain–hindbrain barrier), eye, otic vesicle, somites, and tailbud (Figures 5P,P' and S4U,V). Additional staining was observed in the heart, hatching gland, and posterior notochord at 48 hpf (Figures 5Q,Q' and S4W–Y), and in the epidermis, jaws, pharyngeal arch, cloaca, and fin rays at 4 dpf (Figures 5R,R' and S4Z,Z').

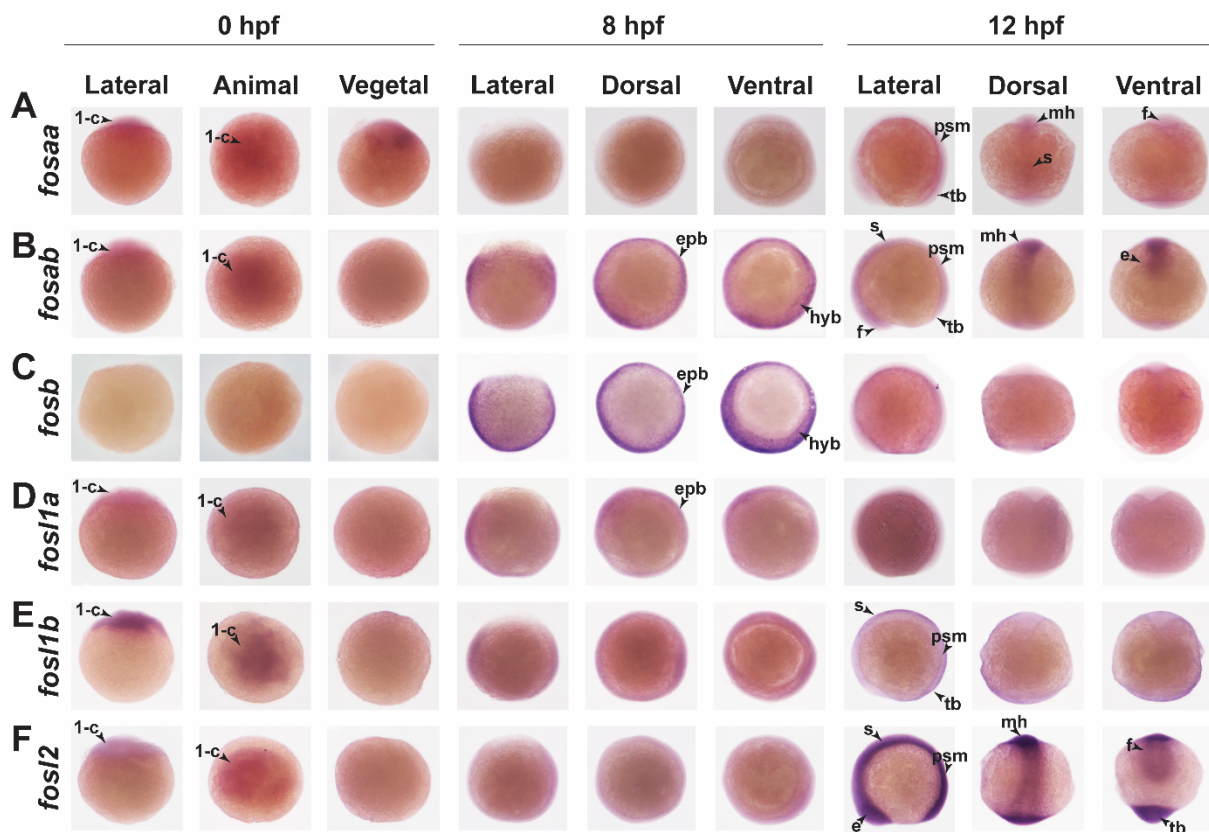


Figure 4. Spatiotemporal expression of *fos* genes during early zebrafish embryonic development. Lateral, dorsal, and frontal views of 0 hpf, 8 hpf, and 12 hpf zebrafish embryos analysed by WISH showing expression for *fosaa* (A), *fosab* (B), *fosb* (C), *fosl1a* (D), *fosl1b* (E), and *fosl2* (F). 1-c, one cell; e, eye; epb, epiblast; f, forebrain; hyb, hypoblast; mh, mid and hindbrain; psm, presomitic mesoderm; s, somite; tb, tailbud. Black arrows within each panel point to the specific expression indicated by the abbreviation.

2.4. Expression of FOS Genes in Adult Zebrafish Tissues

To determine the levels of *fosaa*, *fosab*, *fosb*, *fosl1a*, *fosl1b*, and *fosl2* transcripts in adult male and female zebrafish tissues, we performed qRT-PCR analysis (Figure 6) using optimised primers (Figure S3). In male zebrafish, all *fos* genes displayed weak expression in the heart and liver (Figure 6A–F). All *fos* genes showed high expression in the brain, particularly *fosb*, *fosl1b*, and *fosl2*. All *fos* genes were expressed in the spleen, where *fosb* and

fosl1b levels were highest. In the intestine, *fosab*, *fosb*, and *fosl1b* levels were high, whereas *fosaa*, *fosl1a*, and *fosl2* showed modest expression (Figure 6). Low to moderate level of *fos* gene transcripts were observed for other tissues examined (eyes, kidney, skin, gills, and testis) (Figure 6).

Overall, the expression of *fosaa*, *fosab*, *fosb*, *fosl1a*, *fosl1b*, and *fosl2* was similar in adult zebrafish female tissues, but with modest variations compared to males (Figure 6A–F). All *fos* genes were weakly expressed in the liver of females, whereas *fosl1a* and *fosl1b* showed highest expression in the brain (Figure 6D,E). *fosb* and *fosl1b* showed moderate expression in the spleen, skin, and gills (Figure 6C,E). Amongst *fos* genes, *fosl1b* shows highest expression in the zebrafish adult female intestine (Figure 5E), followed by *fosl2* and *fosl1a*, which shows moderate expression (Figure 6D,F). Moderate to low *fos* expression levels were observed in all other female tissues, including eyes, kidney, gills, spleen, and oocytes (Figure 6A–F).

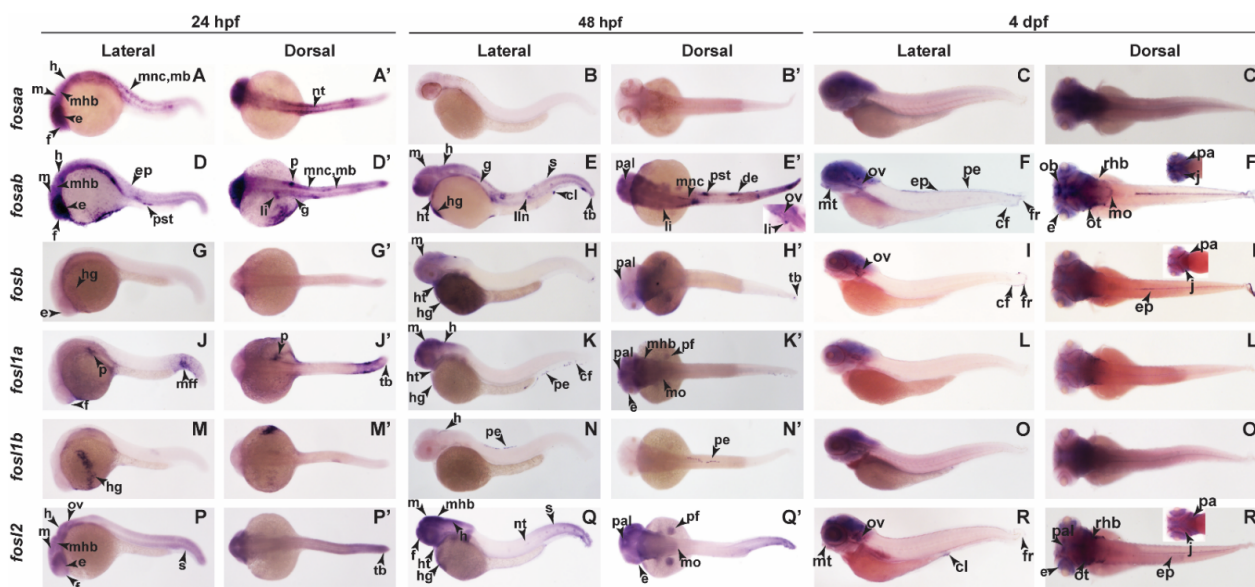


Figure 5. Spatiotemporal expression of *fos* genes in later stages of zebrafish embryonic development. Lateral and dorsal views of zebrafish embryos analysed by WISH showing expression for *fosaa* at 24 hpf (A,A'), 48 hpf (B,B'), and 4 dpf (C,C'); *fosab* at 24 hpf (D,D'), 48 hpf (E,E'), and 4 dpf (F,F'); *fosb* at 24 hpf (G,G'), 48 hpf (H,H'), and 4 dpf (I,I'); *fosl1a* at 24 hpf (J,J'), 48 hpf (K,K'), and 4 dpf (L,L'); *fosl1b* at 24 hpf (M,M'), 48 hpf (N,N'), and 4 dpf (O,O') and *fosl2* at 24 hpf (P,P'), 48 hpf (Q,Q'), and 4 dpf (R,R'). cf, caudal fin; cl, cloaca; de, distal early of nephron; e, eye; ep, epidermis; f, forebrain; fr, fin ray; g, gut; h, hindbrain; hg, hatching gland; ht, heart; j, jaw; li, liver; lln, lateral line neuromasts; m, midbrain; mb, melanoblast; mff, median fin fold; mhb, midbrain hind brain barrier; mnc, migratory neural crest cell; mo, medulla oblongata; mt, mouth; nt, notochord; ob, olfactory bulb; ot, optic tectum; ov, otic vesicle; p, pancreas; pa, pharyngeal arches; pal, pallium; pe, peridermis; pf, pectoral fin; pnc, posterior notochord; pst, proximal straight tubule of nephron; rhb, rostral hindbrain; s, somite; tb, tailbud. Black arrows within each panel point to the specific expression indicated by abbreviations.

2.5. Fos Genes Are Induced in BRAF-Driven Melanoma in Zebrafish

The ERK MAPK pathway is a key signalling pathway regulating the transcription of human *Fos* genes [1]. To determine if this pathway also regulates expression of zebrafish *Fos* genes, we expressed the human BRAF^{V600E} to drive ERK MAPK activation in zebrafish melanocytes using the MiniCoopR transgenesis system [36], which allows rapid testing of candidate modifiers of melanoma development in F0 zebrafish generation (Figure 7A,B). Gene expression analysis on zebrafish melanoma samples revealed higher transcript levels of all *fos* genes except *fosl1b*, with *fosb* displaying the highest relative expression (Figure 7C). These findings indicate functional conservation of *fos* gene regulation by the ERK MAPK pathway in zebrafish.

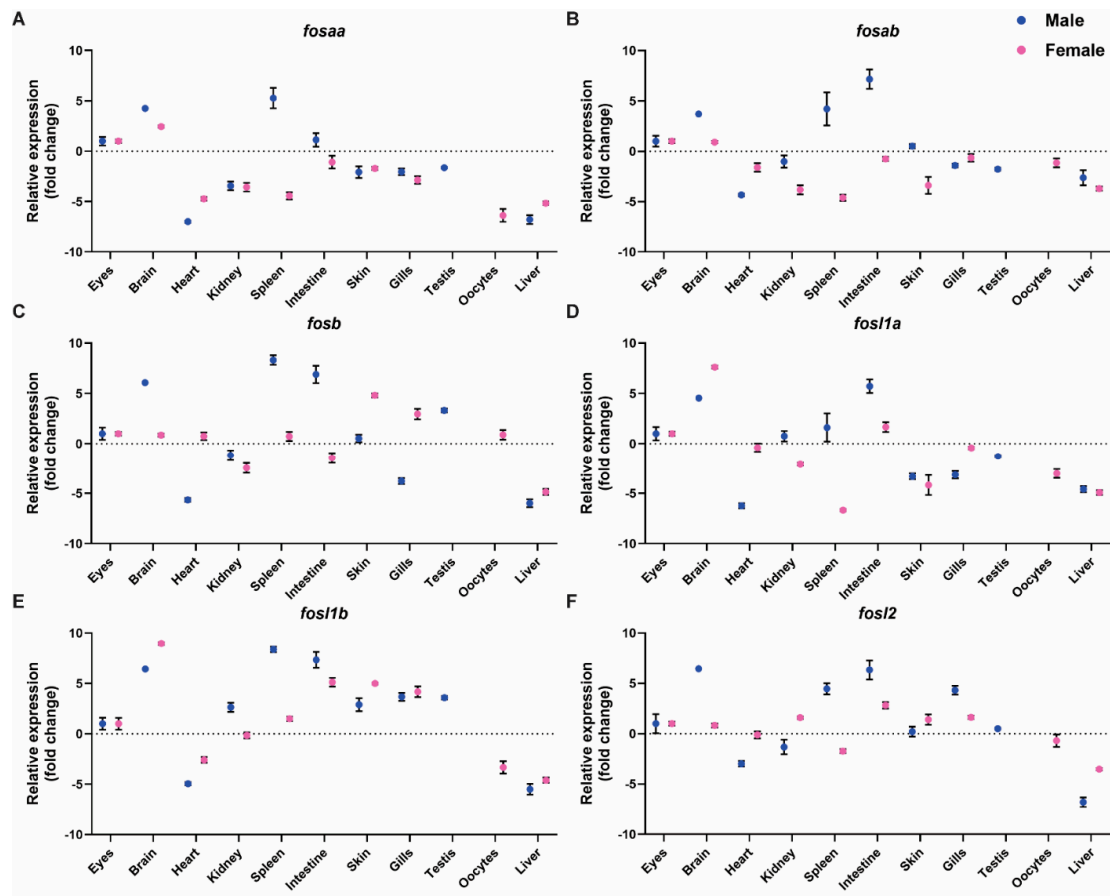


Figure 6. Relative expression of *fos* genes in male and female zebrafish adult tissues. mRNA expression levels of *fosaa* (A), *fosab* (B), *fosb* (C), *fosl1a* (D), *fosl1b* (E), and *fosl2* (F) in zebrafish adult male tissues eyes, brain, heart, kidney, spleen, intestine, skin, gills, testis, and liver were determined by qRT-PCR. The relative mRNA levels were normalised to *actb* and *ddct* values determined by comparison with expression in the male eyes, the tissue with moderate expression. The black error bars indicate the standard error of mean for four biological replicates and the dotted line indicates the median in a tissue showing moderate expression.

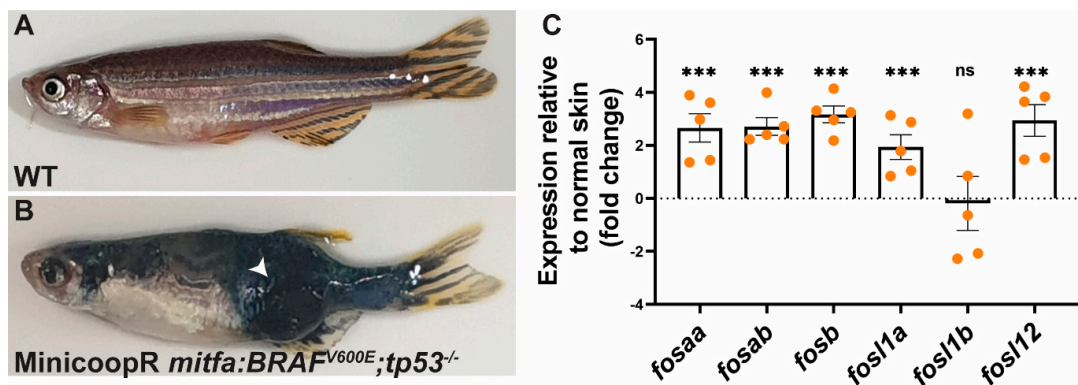


Figure 7. Relative expression of *fos* genes in human BRAF^{V600E} oncogene driven melanoma in zebrafish. mRNA expression levels of zebrafish *fos* genes were determined in normal wildtype (WT) skin (A) and melanoma tumour from BRAF^{V600E}; *tp53*^{-/-} zebrafish line (B), with the graph showing the expression relative to the normal skin (fold change) (C). The relative mRNA levels were normalised to *actb* and *ddct* values determined by comparison with expression in the normal wildtype skin. Error bars indicate the standard error of mean for five biological replicates with statistical significance indicated (***) $p < 0.001$, ns not significant). The white arrow indicates the tumour.

3. Discussion

Despite their well-documented roles as key regulators of cell fate in a multitude of normal and pathological contexts, several important aspects of FOS protein biology remain poorly understood, particularly *in vivo*, such as how specific FOS heterodimers regulate transcription and how their activities are regulated. Though possible, such studies are challenging to undertake in mice, the main *in vivo* model that has been used to study FOS protein biology. Our findings highlight the potential of zebrafish as a vertebrate model for such studies.

The six zebrafish FOS proteins share 40–65% sequence identity and 56–74% similarity to their respective human counterparts. As expected, sequence conservation was highest in the respective bZIP domains of zebrafish and human FOS proteins. However, we also found that zebrafish Fos proteins retained significant sequence conservation in other functional domains previously identified in human FOS isoforms [1], including the N- and C-terminal transcription activation domains of c-FOS and FOSB, and the C-terminal DEST that controls protein stability. The exception was *Fosl1b*, which lacked a C-terminal region, including the DEST domain. As FOS proteins are stabilised upon deletion or ERK pathway-dependent phosphorylation of this domain [15,17], it is likely that *Fosl1b* is inherently more stable than the other zebrafish FOS orthologs and that its expression is uncoupled from ERK pathway regulation. Such divergence has often been observed in paralogs arising from gene duplication events [37] and provides an evolutionary mechanism for creating unique protein functionalities.

The major mechanism of FOS protein regulation is through post-translational modification, primarily phosphorylation. We found that phosphorylation sites previously identified in human FOS proteins [1] are also conserved in zebrafish. Thus, the functionality of each FOS isoform is likely to be regulated via similar mechanisms in both species. Additionally, the conservation of regulatory elements, including phosphorylation sites, suggests that their functional impacts could be characterised *in vivo* using targeted genome editing approaches in zebrafish.

One of the least understood aspects of FOS biology is their roles during early embryonic development. Compared to mice, such investigations are much easier to undertake in zebrafish, as they have transparent embryos, develop externally, and are readily amenable to genetic manipulation. Our data suggest that zebrafish *fos* genes play distinct and temporally restricted roles in specific cell lineages and tissues during early development. For example, whereas sustained *fosab* and *fosl2* expression was evident over 4 days of development in multiple lineages, *fosaa*, *fosl1a*, and *fosl1b* showed more transient expression. The pattern of *fosab* expression suggests it may play a role during early development of embryonic skin, liver, and pancreas. In addition to *fosab*, *fosl1a* also may play roles in pancreatic development. Interestingly, all *fos* genes except *fosl1b* showed transient expression in the embryonic eyes and brain, indicating potential roles for *fos* genes in development of these tissues. Expression of *fosab*, *fosb*, and *fosl2* in the jaws and pharyngeal arches suggests these genes may participate in bone and cartilage development, as has been previously reported in mice [27,38]. In addition to their distinct expression patterns in the early embryo, we found that *fos* genes were expressed in a variety of adult zebrafish tissues. Interestingly, *fos* gene expression appears to differ between some male and female tissues, most notably the spleen. This finding suggests a potential role for *fos* genes in regulating sexual dimorphism in the immune system, a possibility that warrants further investigation. Of note expression of *fos* has previously been shown to be sexually dimorphic in the zebrafish brain [39].

The data from our WISH analysis highlight the potential of zebrafish as an alternative *in vivo* model to mice for investigating the roles of Fos proteins in vertebrates. An important goal of future studies will be to use the powerful toolkit available for genetic manipulation in zebrafish to dissect the role of specific *fos* genes in the embryo. To date, few such analyses have been undertaken with the exception of the heart, where *fosl2* was reported to potentiate the rate of myocardial differentiation from the zebrafish second heart field [40] and where cardiomyocyte-specific expression of a dominant negative AP-1 protein leads to defects in

cardiomyocyte proliferation following injury [41]. Consistent with these observations, we also noted expression of *fosl2*, as well as *fosab*, *fosb*, and *fosl1a*, in the embryonic heart.

In mammalian cells, Fos genes are classified as inducible immediate early genes transiently induced by extracellular signals such as growth factors, hormones, and cytokines [42]. Though limited, available evidence indicates that they are also likely to be inducible genes in zebrafish. For example, expression of zebrafish c-Fos orthologs has been shown to be induced in the dorsal telencephalon by cannabinoids [43]. *Fosl1a* was induced during skeletal muscle regeneration [44] while *fosab*, *fosl1a*, and *fosl2* were induced during heart regeneration [45]. The major pathway regulating transcription of Fos genes in mammalian cells is the ERK MAPK pathway, whose activation in response to IGF and FGF signalling has been shown to control key developmental events in zebrafish embryos, including somite boundary formation [46], dorsoventral patterning [47], axial patterning [48], and the development of the subpallial telencephalon [49]. Interestingly, we found that *fosaa*, *fosab*, *fosl1b*, and *fosl2* were expressed in the presomitic mesoderm, where ERK signalling has been shown to be critical for somitogenesis in both zebrafish and chick embryos [50]. In addition to developmental contexts, ERK signalling has also been reported to induce FOS gene expression downstream of oncogenic lesions, such as activating mutations in the BRAF gene, which frequently occur in human melanomas [51–54]. Consistent with these observations, we show that *fos* gene expression was also induced in zebrafish BRAF mutant melanomas, indicating functional conservation of key pathways regulating expression of these genes in humans and zebrafish. Thus, zebrafish may provide a useful model to dissect the role of specific Fos genes during development and progression of melanoma and other oncogene-driven cancers.

4. Materials and Methods

4.1. Identification of Zebrafish FOS Family Orthologues

Zebrafish orthologues of human FOS genes were identified by bioinformatics analysis using the National Centre for Biotechnology Information (<https://www.ncbi.nlm.nih.gov/>, accessed on 9 May 2022) and the Zebrafish Information Network (<https://zfin.org/>, accessed on 9 May 2022). The FASTA sequences of human FOS mRNAs were obtained from the NCBI database and used for Basic Local Alignment Search Tool (BLAST) (<https://blast.ncbi.nlm.nih.gov/Blast.cgi>, accessed on 9 May 2022) analysis to identify the zebrafish orthologues which were further crosschecked with the ZFIN database and confirmed by sanger sequencing.

4.2. Multiple Sequence Alignment (MSA) and Phylogenetic Comparison of FOS Family Orthologues in Human and Zebrafish

Sequence comparisons of human and zebrafish FOS protein orthologues were determined using pBLAST. Multiple sequence alignments (MSA) were performed using Clustal X version 2.1 software and bootstrapped phylogenetic trees of 1000 replicates generated using the neighbor-joining algorithm [55], then visualised in TreeView [56]. The genomic arrangement of human and zebrafish FOS gene loci, including syntenic genes, was determined using NCBI Map Viewer. Information on regulatory phosphorylation sites in human FOS proteins was obtained from the Phosphosite database (www.phosphosite.org, accessed on 9 May 2022). Synteny analysis for zebrafish and human *FOSL1* and *FOSL2* genes was performed using the Genomicus database [57].

4.3. Zebrafish Maintenance and Embryo Collection

Zebrafish were maintained under standard husbandry practices [39], following the national guidelines for animal use and care, with approval from the Deakin University Animal Welfare Committee. Embryos were collected manually and nurtured in a petri dish containing E3 media and incubated at 28.5 °C, with transparency maintained by adding 0.003% (*w/v*) 1-phenyl-2-thio-urea (PTU), a pigment inhibitor into the E3 media from 9 h post fertilization (hpf).

4.4. Quantitative Real-Time Polymerase Chain Reaction (qRT-PCR)

Adult zebrafish were euthanised with benzocaine and their tissues were isolated by dissection. Total RNA was extracted using RNeasy Mini Kit (Qiagen) according to the manufacturer's guidelines. qRT-PCR was performed using the iTaq™ Universal SYBRGreen Supermix (Biorad, South Granville, Australia) according to the manufacturer's guidelines with the following primers: *fosaa* (5'-AACATCAAGAAGCGAGGCGT, 5'-CGGAGACTCGCCCTGTGC), *fosab* (5'-CGATACACTGCAAGCTGAAAC, 5'-CGGCGA GGATGAACTCTAAC), *fosb* (5'-GTCAAAGTGGCACGGGCT, 5'-GGTCAGCGTTTCATCTC GTG), *fosl1a* (5'-CACAACCCAACAACAACAGAAG, 5'-GGAGGGCTGAGGAGGATTC), *fosl1b* (5'-TCAAACCCGCAAGTCACCTC, 5'-ATCTATGCTGGTTGTGAATGAC), *fosl2* (5'-GACACTGGTCTGTTGGGAAT, 5'-TACTTCTGGTAACTGGAGGCG), and *actb* (5'-TGGCATCACACCTTCTAC, 5'-AGACCATCACCAGAGTCC). Standard and unknown samples were assayed in triplicate using the following thermocycle profile conditions: initial incubation at 95 °C for 5 s, 58 °C for 10 s, and then 72 °C for 20 s. Data was normalized to *actb* and the relative fold changes in adult male and female zebrafish tissue gene expression were determined by comparison with the expression in the male eyes (tissue with moderate overall *fos* gene expression) by using the ddct method [58].

4.5. Whole-Mount In Situ Hybridization (WISH)

Total RNA was isolated from zebrafish embryos using TRIsure (Bioline) according to the manufacturer's instructions and cDNA synthesis was performed using an iScript cDNA synthesis kit (Promega). RT-PCR was performed to amplify cDNA by using the Go Taq Green Master Mix (Promega, Madison, USA) using the following primers: *fosaa* (5'-GGAAGAGCAAGAGCGAGCA, 5'-CTTGTAGAGCGTCTCCCAGTC), *fosab* (5'-TGACA GGATGATGTTTACCAGC, 5'-CGGCTCCAGGTCAGTGTTAG), *fosb* (5'-ACAGTAGGTGTT TCGGCTTCTC, 5'-GGTGGTGGGATGAGTAGGC), *fosl1a* (5'-AAACGCCAGCAGAGAGTGTC, 5'-GGTAAATGGAGTCAGGGATGG), *fosl1b* (5'-ACACCAACCAGCCACGAAAC, 5'-CGG GAATCATAATACGACTCTC), and *fosl2* (5'-TGTCGGAACCGCAGAAGAG, 5'-ATCTCTC CTCTGGCTTTACCTTC). PCR reactions were performed under the following conditions for 35 cycles: 2 min at 95 °C, 30 s at 95 °C, 30 s at 55 °C, 1.5 min at 72 °C, and 10 min at 72 °C. RT-PCR amplified cDNA products of *fosaa*, *fosab*, *fosb*, *fosl1a*, *fosl1b*, and *fosl2* were isolated, purified and cloned into pGEM-T Easy vectors. Purified plasmids with the gene insert were linearised, followed by transcription using either T7 or SP6 polymerase and DIG RNA labelling mix (Roche) to generate DIG-labelled anti-sense and sense probes, which was followed by their purification using Probe-Quant G-50 micro columns (Cytiva). At different time points during development, embryos were collected, dechorionated, and anesthetized with 0.4 mg/mL benzocaine before fixing with 4% *w/v* paraformaldehyde (PFA) at 4 °C. WISH was performed using digoxigenin (DIG)-labelled RNA probes as described in [38] and the images were obtained using an Olympus MVX10 monozoom microscope with a 1 × MVXPlan Aplan lens (NA = 0.25) with an Olympus DP74 camera. Specific expression of each probe was confirmed by comparison to their corresponding sense controls.

4.6. Melanoma Model

Zebrafish melanoma formation was studied as described previously [36]. Briefly, 25 pg of a MiniCoopR vector expressing BRAF^{V600E} (MiniCoopR mitfa:BRAF^{V600E}) was microinjected along with 25 pg of Tol2 transposase mRNA into one-cell stage *tp53* knockout embryos. The animals were monitored weekly for the presence of visible tumours. The tumours were dissected and RNA extracted for subsequent qRT-PCR analysis to determine the expression of zebrafish *fos* genes.

Supplementary Materials: The following supporting information can be downloaded at: <https://www.mdpi.com/article/10.3390/ijms231710098/s1>.

Author Contributions: Conceptualization, F.B. and A.S.D.; methodology, K.K., F.B., G.K.G. and S.H.; validation, K.K., F.B. and A.S.D.; formal analysis, K.K., F.B., A.S.D. and A.C.W.; investigation, K.K., F.B., A.S.D. and A.C.W.; resources, A.S.D. and F.B.; data curation, F.B. and K.K.; writing, original draft preparation, F.B., A.S.D. and A.C.W.; writing, review and editing, F.B., A.S.D., A.C.W. and C.L.; supervision, F.B. and A.S.D.; project administration, F.B. and A.S.D.; funding acquisition, F.B. and A.S.D. All authors have read and agreed to the published version of the manuscript. All authors contributed to data interpretation and drafting of the paper, and all approved the final manuscript.

Funding: This project was supported by National Health and Medical Research Council grant 1141906 and IMPACT Seed Funding from Deakin University, Australia.

Institutional Review Board Statement: This study was approved by the Deakin University Animal Ethics Committee under projects G13-2019 (29 August 2019) and G21-2019 (15 June 2020).

Informed Consent Statement: Not applicable.

Data Availability Statement: All data generated or analyzed during this study are included in this published article (and its Supplementary Materials).

Acknowledgments: This work was supported by grants from the National Health and Medical Research Council of Australia and from Deakin University (IMPACT). The authors also acknowledge the exceptional support provided by the Deakin University Animal Facility staff. We also thank members of the Zon Lab, Leonard Zon, Haley Noonan, Alicia McConell, and Georgia Stirtz for reagents and advice on the zebrafish melanoma model.

Conflicts of Interest: The authors declare that they have no competing interests.

References

1. Tulchinsky, E. Fos family members: Regulation, structure and role in oncogenic transformation. *Histol. Histopathol.* **2000**, *15*, 921–928. [[PubMed](#)]
2. Bejjani, F.; Evanno, E.; Zibara, K.; Piechaczyk, M.; Jariel-Encontre, I. The AP-1 transcriptional complex: Local switch or remote command? *Biochim. Biophys. Acta (BBA)-Rev. Cancer* **2019**, *1872*, 11–23. [[CrossRef](#)] [[PubMed](#)]
3. Jochum, W.; Passequé, E.; Wagner, E.F. AP-1 in mouse development and tumorigenesis. *Oncogene* **2001**, *20*, 2401–2412. [[CrossRef](#)] [[PubMed](#)]
4. Shaulian, E.; Karin, M. AP-1 as a regulator of cell life and death. *Nat. Cell Biol.* **2002**, *4*, E131–E136. [[CrossRef](#)] [[PubMed](#)]
5. Shaulian, E.; Karin, M. AP-1 in cell proliferation and survival. *Oncogene* **2001**, *20*, 2390–2400. [[CrossRef](#)]
6. Angel, P.; Szabowski, A.; Schorpp-Kistner, M. Function and regulation of AP-1 subunits in skin physiology and pathology. *Oncogene* **2001**, *20*, 2413–2423. [[CrossRef](#)]
7. Chinenov, Y.; Kerppola, T.K. Close encounters of many kinds: Fos-Jun interactions that mediate transcription regulatory specificity. *Oncogene* **2001**, *20*, 2438–2452. [[CrossRef](#)]
8. Macian, F.; López-Rodríguez, C.; Rao, A. Partners in transcription: NFAT and AP-1. *Oncogene* **2001**, *20*, 2476–2489. [[CrossRef](#)]
9. Van Dam, H.; Castellazzi, M. Distinct roles of Jun: Fos and Jun: ATF dimers in oncogenesis. *Oncogene* **2001**, *20*, 2453–2464. [[CrossRef](#)]
10. Trop-Steinberg, S.; Azar, Y. AP-1 expression and its clinical relevance in immune disorders and cancer. *Am. J. Med. Sci.* **2017**, *353*, 474–483. [[CrossRef](#)]
11. Eferl, R.; Wagner, E.F. AP-1: A double-edged sword in tumorigenesis. *Nat. Rev. Cancer* **2003**, *3*, 859–868. [[CrossRef](#)] [[PubMed](#)]
12. Wisdom, R.; Verma, I.M. Transformation by Fos proteins requires a C-terminal transactivation domain. *Mol. Cell. Biol.* **1993**, *13*, 7429–7438. [[PubMed](#)]
13. Sutherland, J.A.; Cook, A.; Bannister, A.J.; Kouzarides, T. Conserved motifs in Fos and Jun define a new class of activation domain. *Genes Dev.* **1992**, *6*, 1810–1819. [[CrossRef](#)]
14. Wisdom, R.; Yen, J.; Rashid, D.; Verma, I.M. Transformation by FosB requires a trans-activation domain missing in FosB2 that can be substituted by heterologous activation domains. *Genes Dev.* **1992**, *6*, 667–675. [[CrossRef](#)] [[PubMed](#)]
15. Gomard, T.; Jariel-Encontre, I.; Basbous, J.; Bossis, G.; Mocquet-Torcy, G.; Piechaczyk, M. Fos family protein degradation by the proteasome. *Biochem. Soc. Trans.* **2008**, *36 Pt 5*, 858–863. [[CrossRef](#)]
16. Pakay, J.L.; Diesch, J.; Gilan, O.; Yip, Y.Y.; Sayan, E.; Kolch, W.; Mariadason, J.M.; Hannan, R.D.; Tulchinsky, E.; Dhillon, A.S. A 19S proteasomal subunit cooperates with an ERK MAPK-regulated degron to regulate accumulation of Fra-1 in tumour cells. *Oncogene* **2012**, *31*, 1817–1824. [[CrossRef](#)]
17. Sayan, A.E.; Stanford, R.; Vickery, R.; Grigorenko, E.; Diesch, J.; Kulbicki, K.; Edwards, R.; Pal, R.; Greaves, P.; Jariel-Encontre, I.; et al. Fra-1 controls motility of bladder cancer cells via transcriptional upregulation of the receptor tyrosine kinase AXL. *Oncogene* **2012**, *31*, 1493–1503. [[CrossRef](#)]

18. Hess, J.; Angel, P.; Schorpp-Kistner, M. AP-1 subunits: Quarrel and harmony among siblings. *J. Cell Sci.* **2004**, *117*, 5965–5973. [[CrossRef](#)]
19. Angel, P.; Karin, M. The role of Jun, Fos and the AP-1 complex in cell-proliferation and transformation. *Biochim. Biophys. Acta (BBA)-Rev. Cancer* **1991**, *1072*, 129–157. [[CrossRef](#)]
20. Reichmann, E.; Schwarz, H.; Deiner, E.M.; Leitner, I.; Eilers, M.; Berger, J.; Busslinger, M.; Beug, H. Activation of an inducible c-FosER fusion protein causes loss of epithelial polarity and triggers epithelial-fibroblastoid cell conversion. *Cell* **1992**, *71*, 1103–1116. [[CrossRef](#)]
21. Saez, E.; Rutberg, S.E.; Mueller, E.; Oppenheim, H.; Smoluk, J.; Yuspa, S.H.; Spiegelman, B.M. c-Fos is required for malignant progression of skin tumors. *Cell* **1995**, *82*, 721–732. [[CrossRef](#)]
22. Mahner, S.; Baasch, C.; Schwarz, J.; Hein, S.; Wölber, L.; Jänicke, F.; Milde-Langosch, K. C-Fos expression is a molecular predictor of progression and survival in epithelial ovarian carcinoma. *Br. J. Cancer* **2008**, *99*, 1269–1275. [[CrossRef](#)] [[PubMed](#)]
23. Guo, J.-C.; Li, J.; Zhao, Y.-P.; Zhou, L.; Cui, Q.-C.; Zhou, W.-X.; Zhang, T.P.; You, L. Expression of c-fos was associated with clinicopathologic characteristics and prognosis in pancreatic cancer. *PLoS ONE* **2015**, *10*, e0120332. [[CrossRef](#)]
24. Funk, M.; Poensgen, B.; Graulich, W.; Jérôme, V.; Müller, R. A novel, transformation-relevant activation domain in Fos proteins. *Mol. Cell. Biol.* **1997**, *17*, 537–544. [[CrossRef](#)]
25. Tkach, V.; Tulchinsky, E.; Lukanidin, E.; Vinson, C.; Bock, E.; Berezin, V. Role of the Fos family members, c-Fos, Fra-1 and Fra-2, in the regulation of cell motility. *Oncogene* **2003**, *22*, 5045–5054. [[CrossRef](#)] [[PubMed](#)]
26. Dhillon, A.S.; Tulchinsky, E. FRA-1 as a driver of tumour heterogeneity: A nexus between oncogenes and embryonic signalling pathways in cancer. *Oncogene* **2015**, *34*, 4421–4428. [[CrossRef](#)] [[PubMed](#)]
27. Wagner, E. Functions of AP1 (Fos/Jun) in bone development. *Ann. Rheum. Dis.* **2002**, *61* (Suppl. S2), ii40–ii42. [[CrossRef](#)]
28. Wang, Z.-Q.; Ovitt, C.; Grigoriadis, A.E.; Möhle-Steinlein, U.; Rüther, U.; Wagner, E.F. Bone and haematopoietic defects in mice lacking c-fos. *Nature* **1992**, *360*, 741–745. [[CrossRef](#)]
29. Grigoriadis, A.E.; Schellander, K.; Wang, Z.-Q.; Wagner, E.F. Osteoblasts are target cells for transformation in c-fos transgenic mice. *J. Cell Biol.* **1993**, *122*, 685–701. [[CrossRef](#)]
30. Brown, J.R.; Ye, H.; Bronson, R.T.; Dikkes, P.; Greenberg, M.E. A defect in nurturing in mice lacking the immediate early gene fosB. *Cell* **1996**, *86*, 297–309. [[CrossRef](#)]
31. Kent, L.N.; Rumi, M.K.; Kubota, K.; Lee, D.-S.; Soares, M.J. FOSL1 is integral to establishing the maternal-fetal interface. *Mol. Cell. Biol.* **2011**, *31*, 4801–4813. [[CrossRef](#)]
32. Renaud, S.J.; Kubota, K.; Rumi, M.K.; Soares, M.J. The FOS transcription factor family differentially controls trophoblast migration and invasion. *J. Biol. Chem.* **2014**, *289*, 5025–5039. [[CrossRef](#)]
33. Marrs, J.A.; Sarmah, S. The Genius of the Zebrafish Model: Insights on Development and Disease. *Biomedicines* **2021**, *9*, 577. [[CrossRef](#)] [[PubMed](#)]
34. Saitou, N.; Nei, M. The neighbor-joining method: A new method for reconstructing phylogenetic trees. *Mol. Biol. Evol.* **1987**, *4*, 406–425. [[PubMed](#)]
35. Perriere, G.; Gouy, M. WWW-query: An on-line retrieval system for biological sequence banks. *Biochimie* **1996**, *78*, 364–369. [[CrossRef](#)]
36. Nguyen, N.T.T.; Vincens, P.; Dufayard, J.F.; Crollius, H.R.; Louis, A. Genomicus in 2022: Comparative tools for thousands of genomes and reconstructed ancestors. *Nucleic Acids Res.* **2022**, *50*, D1025–D1031. [[CrossRef](#)]
37. Livak, K.J.; Schmittgen, T.D. Analysis of relative gene expression data using real-time quantitative PCR and the 2(-Delta Delta C(T)) Method. *Methods* **2001**, *25*, 402–408. [[CrossRef](#)]
38. Thisse, C.; Thisse, B. High-resolution in situ hybridization to whole-mount zebrafish embryos. *Nat. Protoc.* **2008**, *3*, 59–69. [[CrossRef](#)]
39. Ceol, C.J.; Houvras, Y.; Jane-Valbuena, J.; Bilodeau, S.; Orlando, D.A.; Battisti, V.; Fritsch, L.; Lin, W.M.; Hollmann, T.J.; Ferré, F.; et al. The histone methyltransferase SETDB1 is recurrently amplified in melanoma and accelerates its onset. *Nature* **2011**, *471*, 513–517. [[CrossRef](#)]
40. Weidenfeld-Baranboim, K.; Bitton-Worms, K.; Aronheim, A. TRE-dependent transcription activation by JDP2–CHOP10 association. *Nucleic Acids Res.* **2008**, *36*, 3608–3619. [[CrossRef](#)]
41. Aronheim, A.; Zandi, E.; Hennemann, H.; Elledge, S.J.; Karin, M. Isolation of an AP-1 repressor by a novel method for detecting protein-protein interactions. *Mol. Cell. Biol.* **1997**, *17*, 3094–3102. [[CrossRef](#)] [[PubMed](#)]
42. Bozec, A.; Bakiri, L.; Jimenez, M.; Schinke, T.; Amling, M.; Wagner, E.F. Fra-2/AP-1 controls bone formation by regulating osteoblast differentiation and collagen production. *J. Cell Biol.* **2010**, *190*, 1093–1106. [[CrossRef](#)] [[PubMed](#)]
43. Lee, S.L.; Horsfield, J.A.; Black, M.A.; Rutherford, K.; Gemmell, N.J. Identification of sex differences in zebrafish (*Danio rerio*) brains during early sexual differentiation and masculinization using 17 α -methyltestosterone. *Biol. Reprod.* **2018**, *99*, 446–460. [[CrossRef](#)] [[PubMed](#)]
44. Jahangiri, L.; Sharpe, M.; Novikov, N.; Gonzalez-Rosa, J.M.; Borikova, A.; Nevis, K.; Paffett-Lugassy, N.; Zhao, L.; Adams, M.; Guner-Ataman, B.; et al. The AP-1 transcription factor component Fosl2 potentiates the rate of myocardial differentiation from the zebrafish second heart field. *Development* **2016**, *143*, 113–122. [[CrossRef](#)]

45. Beisaw, A.; Kuenne, C.; Guenther, S.; Dallmann, J.; Wu, C.C.; Bentsen, M.; Looso, M.; Stainier, D.Y. AP-1 Contributes to Chromatin Accessibility to Promote Sarcomere Disassembly and Cardiomyocyte Protrusion During Zebrafish Heart Regeneration. *Circ. Res.* **2020**, *126*, 1760–1778. [[CrossRef](#)]
46. Murphy, L.O.; Smith, S.; Chen, R.H.; Fingar, D.C.; Blenis, J. Molecular interpretation of ERK signal duration by immediate early gene products. *Nat. Cell Biol.* **2002**, *4*, 556–564. [[CrossRef](#)]
47. Ruhl, T.; Zeymer, M.; von der Emde, G. Cannabinoid modulation of zebrafish fear learning and its functional analysis investigated by c-Fos expression. *Pharmacol. Biochem. Behav.* **2017**, *153*, 18–31. [[CrossRef](#)]
48. Louie, K.W.; Saera-Vila, A.; Kish, P.E.; Colacino, J.A.; Kahana, A. Temporally distinct transcriptional regulation of myocyte dedifferentiation and Myofiber growth during muscle regeneration. *BMC Genom.* **2017**, *18*, 854. [[CrossRef](#)]
49. Goldman, J.A.; Kuzu, G.; Lee, N.; Karasik, J.; Gemberling, M.; Foglia, M.J.; Karra, R.; Dickson, A.L.; Sun, F.; Tolstorukov, M.Y.; et al. Resolving Heart Regeneration by Replacement Histone Profiling. *Dev. Cell* **2017**, *40*, 392–404.e5. [[CrossRef](#)]
50. Sawada, A.; Shinya, M.; Jiang, Y.J.; Kawakami, A.; Kuroiwa, A.; Takeda, H. Fgf/MAPK signalling is a crucial positional cue in somite boundary formation. *Development* **2001**, *128*, 4873–4880. [[CrossRef](#)]
51. Furthauer, M.; Van Celst, J.; Thisse, C.; Thisse, B. Fgf signalling controls the dorsoventral patterning of the zebrafish embryo. *Development* **2004**, *131*, 2853–2864. [[CrossRef](#)] [[PubMed](#)]
52. Tsang, M.; Maegawa, S.; Kiang, A.; Habas, R.; Weinberg, E.; Dawid, I.B. A role for MKP3 in axial patterning of the zebrafish embryo. *Development* **2004**, *131*, 2769–2779. [[CrossRef](#)] [[PubMed](#)]
53. Shinya, M.; Koshida, S.; Sawada, A.; Kuroiwa, A.; Takeda, H. Fgf signalling through MAPK cascade is required for development of the subpallial telencephalon in zebrafish embryos. *Development* **2001**, *128*, 4153–4164. [[CrossRef](#)] [[PubMed](#)]
54. Sari, D.W.K.; Akiyama, R.; Naoki, H.; Ishijima, H.; Bessho, Y.; Matsui, T. Time-lapse observation of stepwise regression of Erk activity in zebrafish presomitic mesoderm. *Sci. Rep.* **2018**, *8*, 4335. [[CrossRef](#)] [[PubMed](#)]
55. Davies, H.; Bignell, G.R.; Cox, C.; Stephens, P.; Edkins, S.; Clegg, S.; Teague, J.; Woffendin, H.; Garnett, M.J.; Bottomley, W.; et al. Mutations of the BRAF gene in human cancer. *Nature* **2002**, *417*, 949–954. [[CrossRef](#)]
56. Comandante-Lou, N.; Baumann, D.G.; Fallahi-Sichani, M. AP-1 transcription factor network explains diverse patterns of cellular plasticity in melanoma cells. *Cell Rep.* **2022**, *40*, 111147. [[CrossRef](#)]
57. Ramsdale, R.; Jorissen, R.N.; Li, F.Z.; Al-Obaidi, S.; Ward, T.; Sheppard, K.E.; Bukczynska, P.E.; Young, R.J.; Boyle, S.E.; Shackleton, M.; et al. The transcription cofactor c-JUN mediates phenotype switching and BRAF inhibitor resistance in melanoma. *Sci. Signal.* **2015**, *8*, ra82. [[CrossRef](#)]
58. Caramel, J.; Papadogeorgakis, E.; Hill, L.; Browne, G.J.; Richard, G.; Wierinckx, A.; Saldanha, G.; Osborne, J.; Hutchinson, P.; Tse, G.; et al. A switch in the expression of embryonic EMT-inducers drives the development of malignant melanoma. *Cancer Cell* **2013**, *24*, 466–480. [[CrossRef](#)]